Hindawi
Advances in Meteorology
Volume 2019, Article ID 9090659, 11 pages
https://doi.org/10.1155/2019/9090659

Research Article

Spatiotemporal Distribution Characteristics of Mesoscale Convective Systems Producing Short-Duration Heavy Rainfall over the Tianshan Mountain Area

Jiangang Li,[1,2] **Lianmei Yang**,[1,2] **Wen Liu**,[1,2] **and Cailian Jiang**[3]

[1]*Institute of Desert and Meteorology, CMA, Urumqi 830002, China*
[2]*Center of Central Asian Atmospheric Science Research, Urumqi 830002, China*
[3]*Wujiaqu Meteorology Bureau, Wujiaqu 831300, China*

Correspondence should be addressed to Jiangang Li; shzljg_qxj@163.com

Received 29 November 2018; Revised 27 January 2019; Accepted 28 February 2019; Published 18 March 2019

Academic Editor: Federico Porcù

Based on hourly precipitation data and FY-2 satellite infrared (IR) digital satellite imagery collected during the warm season from 2005 to 2015 in the Tianshan Mountains and the adjacent areas in Xinjiang, China, the definition of mesoscale convective systems (MCSs) was revised based on short-duration heavy precipitation processes. The spatiotemporal development of MCSs in terms of the initiation, maturation, dissipation, duration, and movement was statistically analyzed. Most mesoscale systems in the area were dominated by meso-β convective systems (M_βCSs), which was in line with the annual heavy precipitation frequency. In meso-α convective systems (M_αCSs), persistent elongated convective systems (PECSs) occurred more commonly than mesoscale convective complexes (MCCs). MCSs were common in summer, with the peak frequency of M_αCS occurrence in June and the peak frequency of M_βCS occurrence mainly in July and August. From the perspective of diurnal variations, MCSs initiated in the late afternoon, developed during the evening, and dissipated before midnight. MCSs in general lasted 6~9 h between June and July and 9~11 h in August. The M_αCSs lasted approximately 14 h, and the M_βCSs lasted from 7 h to 12 h. The development and termination stages of MCSs lasted 3~6 h and 2~7 h, respectively. In low-elevation areas and on the windward slope of the mountains, MCSs initiated more easily and more frequently over the northern and western slopes than that over the southern and eastern slopes. The central area of the Junggar basin hosted the development of MCSs, but the distribution of the convective systems at different scales varied. During the termination stage, these mesoscale systems were mainly located at the basin edges. In terms of tracks, most MCSs moved eastward under the influence of the westerlies and the M_αCSs moved faster but in a more scattered manner than the M_βCSs. Additionally, some unusual tracks appeared because of the effects of the underlying surface topography and environmental wind.

1. Introduction

Mesoscale convective systems (MCSs) are significant rain-producing weather systems with organized convection activity accompanied by severe weather phenomena, such as hail and thunderstorms. Monitoring of these systems is a key issue in nowcasting and short-term forecasts because of the associated short-duration and high-intensity rainstorms.

Since 1980, many studies [1–5] have investigated the structure, evolutionary characteristics, and environmental conditions of mesoscale convective complexes (MCCs) using observational data from weather radar and satellites. Further research on the spatiotemporal distribution of MCSs in different regions around the world has produced deeper insights [6–9] and analyzed the structural characteristics and maintenance mechanisms of MCCs and persistent elongated convective systems (PECSs) [10–13].

In Asia, owing to the influence of the South Asian monsoon and the East Asian monsoon, rainstorm disasters induced by MCSs occur frequently. Therefore, the related

studies were focused on monsoon region [11, 14–17]. However, fewer studies of convection activity in the arid areas of the continental hinterland have been done.

As an arid and semiarid area, Xinjiang, especially the mountainous regions, has experienced frequent short-duration heavy rainfall events in recent years [18]. Owing to the widespread distribution of Gobi and desert surfaces with sparse vegetation and low soil porosity, there was poor water storage capacity in the soil. Additionally, because of the primitive state of the local water facilities, secondary disasters, such as flash floods, mudslides, and landslides, caused by short-duration rainstorms have resulted in heavy casualties and property losses.

Because of their short duration and frequent nocturnal occurrences, MCSs remain poorly studied via conventional observations. With high temporal and spatial resolutions, the Doppler weather radar is a useful tool for the analysis of the vertical structure, dimensions, and intensity of MCSs. However, only 8 operational radar stations are expected to be available. Thus, the available data were limited since MCSs cannot be effectively detected early due to their large probable occurrence area and the complicated landscape in Xinjiang. Compared to the rest of Xinjiang, there is relatively abundant rainfall (300~900 mm annual precipitation) in the Tianshan Mountains [19], but few stations have been established in the mountains to track MCSs in real-time due to the difficult maintenance. Radar scanning can only cover a small part of the area near mountains, so the application of satellite data is important. Geostationary satellite observations have the obvious advantages of restriction-free geographical coverage, large coverage area, and high spatial-temporal resolutions, especially in mountainous regions.

Although the MCSs distribution of Xinjiang has been investigated over a relatively short time span [20, 21], the relationship between the MCSs distribution characteristics and strong convective weather has not been discussed. In this paper, the spatial-temporal features of MCSs associated with short-duration heavy precipitation in Xinjiang were analyzed by using FY-2 blackbody brightness temperature (TBB) products in the past 10 years.

2. Study Area, Data, and Methods

In this study, the research area is located over the Tianshan Mountains and a portion of Xinjiang and includes the Yili River Valley, Bortala Mongol Autonomous Prefecture, southern Tacheng region, and the area along the Tianshan Mountain. The specific range was 73~97°E, 38~46°N (Figure 1), which includes 62 national meteorological stations. The topography of the area was variable and was mainly characterized by mountainous areas.

Hourly precipitation data were collected from April to September during 2005~2015 at the national meteorological stations. TBB data from the FY-2 geostationary satellites were obtained from the National Satellite Meteorological Center of the China Meteorological Administration. The time interval of the data was 1 h. The TBB data were calculated for a subastral point at 105°E using data from different satellites at different times: FY-2C from June 2005 to September 2009, FY-2E from April 2010 to May 2015, and FY-2G from June to September 2015. These data included a total of approximately 45000 data files (partial deletion occurred for certain reasons) with a $0.1^\circ \times 0.1^\circ$ spatial resolution and a 45~165°E, 60°S~60°N extent.

The short-duration heavy precipitation processes were defined as follows: (1) an hourly precipitation (R_h) $\geq 20\ mm \cdot h^{-1}$ and (2) a time interval of greater than 24 hours separating two rainfall events. In accordance with the above definition, a total of 35 processes were filtered out.

The TBB products had to be processed as follows: first, the cloud image was numerically enhanced. Then, the convective clouds were highlighted using appropriate maps. Thus, according to the above criteria, the characteristics of MCSs that influence heavy rainfall, including their shape, minimum TBB value, source region, and spatial-temporal distribution, are then investigated.

The time used in this study was the Coordinated Universal Time (UTC), which is 6 h later than the local standard time (LST) in Xinjiang.

3. MCS Criteria

In general, continuous cold cloud areas, lifespans, shapes, etc. were defined as the criteria of MCCs by Maddox [5] and Augustine and Howard [8], although the cold cloud area has since been revised. In China, the scale classification standard was modified by Ma et al. [17], Orlanski [22], and Fei et al. [23] to include the cloud areas, lifespans, and eccentricities (minor axis/major axis) of these systems in accordance with the investigation results from China and adjacent areas.

Since the scale of meso-γ convective systems (M_γCSs) is less than 20 km, satellite data cannot be used to track and distinguish these features, so meso-α convective systems (M_αCSs) and meso-β convective systems (M_βCSs) are the focus of this paper. According to the specific geographical environment in Xinjiang, the criteria for M_αCSs were taken from the study of Zheng et al. [24]. For M_βCSs, the cloud shield area with a TBB $\leq -32^\circ$C must be greater than $10^3\ km^2$ and the duration must exceed 3 h in this paper. In addition, when the eccentricity of an MCS is between 0.2~0.5 at its maximum areal extent, the feature with an infrared (IR) temperature $\leq -32^\circ$C in the form of a continuous cloud shield was defined as a PECS and a meso-β elongated convective system (M_βECS).

4. Results and Discussion

According to the criteria above, a survey of IR images corresponding to precipitation processes was carried out, and nine M_αCS and twenty-six M_βCS events were obtained. Lists of these events are given in Tables 1 and 2.

4.1. MCS Shape Distribution. According to the MCS criteria, different scales of MCS were statistically analyzed based on their eccentricity, which was calculated by rounding. The results showed that a small number of M_βCSs occurred in the spring (April~May) and autumn (September) and that MCS occurred most frequently in the summer

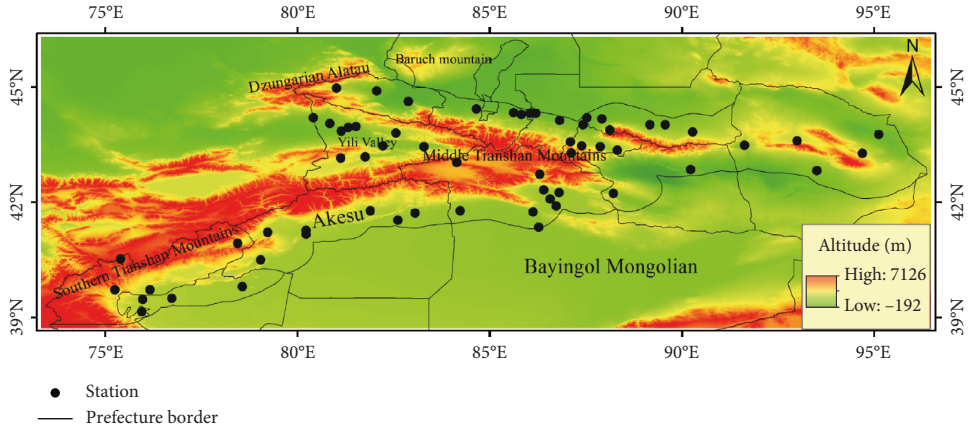

Figure 1: Study area and distribution of weather stations (• represent national meteorological stations).

Table 1: Statistics of the M_αCS occurrences during 2005–2015.

Case no.	Date	Time of maturity	Area of −32°C isotherm (km^2)	Eccentricity
1	**01/06/2006**	**0600**	**229754.0**	**0.71**
2	06/07/2006	1100	262311.3	0.14
3	05/06/2007	0400	104009.6	0.47
4	14/06/2007	0600	380789.3	0.20
5	15/07/2007	2200	369215.3	0.23
6	**18/06/2010**	**0300**	**175098.4**	**0.50**
7	13/06/2011	0600	185631.0	0.30
8	**04/06/2012**	**0200**	**132256.8**	**0.66**
9	**16/06/2013**	**1500**	**168390.1**	**0.76**

Bold represents an MCC.

Table 2: Statistics of the M_βCS occurrences during 2005 to 2015.

Case no.	Date	Time of maturity	Area of −32°C isotherm (km^2)	Eccentricity
1	**04/08/2005**	**0300**	**9518.7**	**0.63**
2	02/07/2006	0000	89745.6	0.46
3	**01/07/2007**	**0300**	**78425.9**	**0.52**
4	**01/08/2007**	**0900**	**93210.0**	**0.88**
5	17/07/2009	0700	18005.9	0.44
6	**04/08/2009**	**0200**	**45662.4**	**0.61**
7	20/06/2010	0300	34217.7	0.32
8	22/06/2010	0200	10779.6	0.39
9	22/06/2010	0300	64891.7	0.38
10	**13/06/2011**	**0300**	**56420.3**	**0.61**
11	17/08/2011	0400	6028.7	0.46
12	**21/06/2012**	**0900**	**17596.3**	**0.56**
13	14/07/2012	0200	1544.1	0.42
14	14/05/2013	0600	57241.3	0.27
15	17/06/2013	1300	93976.5	0.26
16	04/07/2013	2100	35330.7	0.47
17	22/07/2013	0800	17758.1	0.28
18	**25/07/2013**	**0300**	**28614.4**	**0.55**
19	**08/08/2013**	**0500**	**8829.6**	**0.67**
20	**09/08/2013**	**0100**	**15798.6**	**0.61**
21	14/08/2014	1000	25044.1	0.40
22	28/06/2015	0300	55314.0	0.41
23	24/08/2015	1600	39004.4	0.41
24	**01/09/2015**	**1600**	**6328.2**	**0.66**
25	**29/06/2007**	**0800**	**4870.3**	**0.56**
26	07/06/2008	0600	9106.5	0.48

Bold represents an M_βCS.

(June~August). M_αCS and M_βCS events each accounted for 50% of the events in June, and M_βCS event increased markedly in abundance from July to August (Figure 2(a)). PECSs appeared during June and July, while M_βECSs generally occurred from May to September, indicating that elongated convective clouds were more common than their circular counterparts in the Tianshan Mountains. This phenomenon of small eccentricities may be caused by the splitting or merging of clouds over topographically variable mountainous areas.

Figure 2(b) shows that the maximum area distribution of the M_βCS cold cloud shields during their mature period was broad, spanning 10^3~10^4 km^2, and concentrated from 1×10^4 to 5×10^4 km^2. The number of M_βCS events decreases with increasing area. The area distribution of M_αCSs was broader, falling within the span of 1.5×10^5~2×10^5.

4.2. Distribution of TBB_{min}. The brightness temperature of different underlying surfaces can be reflected by the TBB value. The smaller the TBB value in a cloudy area is, the lower the cloud top temperature is and the stronger the convection is. Therefore, the development stage and changes in the intensity of MCSs can be deduced from the TBB value, and this process can provide the basis for quantitative precipitation estimation.

The minimum TBB value of the MCS events corresponding to weather processes was statistically analyzed (Figure 3(a)). TBB_{min} was between −60°C and −42°C, and most values fell within the range of −50~−44°C. These values were slightly higher than the pattern in the northeastern China and comparable to the pattern in eastern China [25, 26], indicating that the development of convection was strong in the mountain areas.

Figure 3(b) shows the frequency of deep convection ($TBB_{min} \le -52$°C represents the deep convection of clouds). Deep convection occurred from May to July and was strongest in June and weaker in the other months, indicating

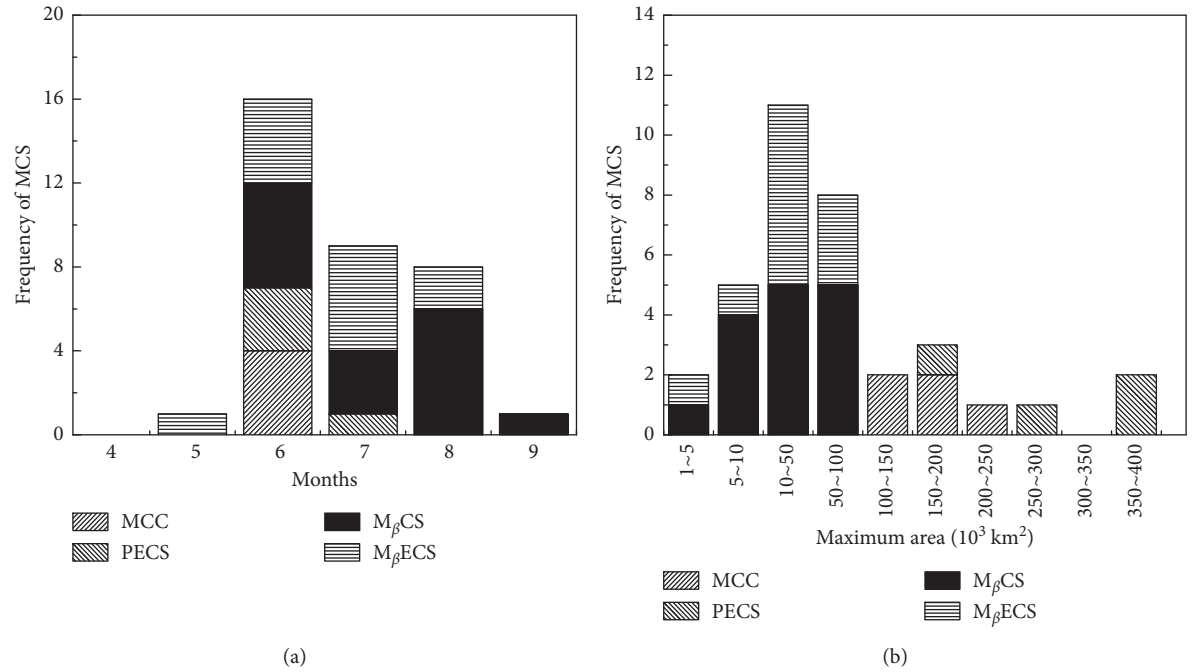

Figure 2: Shape distribution of MCSs by (a) month and (b) area.

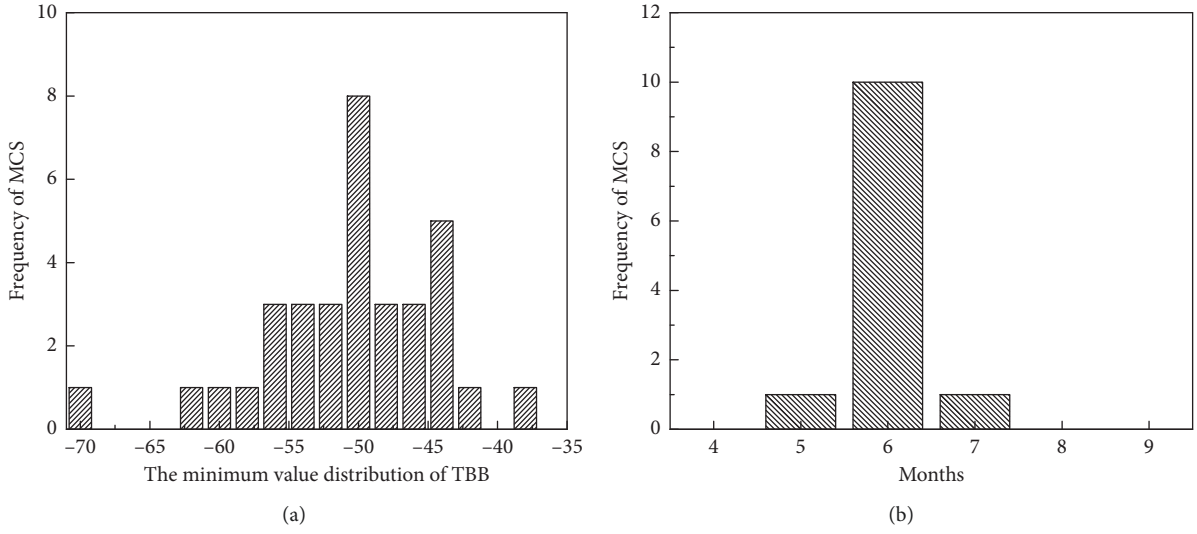

Figure 3: Distribution of (a) TBB_{min} and (b) deep convection in each month.

that June was most likely to experience short-duration heavy rainfall events during the wet season.

4.3. Temporal Distribution of MCSs. From the perspective of annual variations, three maxima appeared in 2007, 2010, and 2013 (Figure 4(a)). Based on the MCS occurrence frequency data, M_βCSs appeared more frequently than M_αCSs, and the pattern of MCSs was basically consistent with that of the number of heavy rain events.

Heavy precipitation processes were most frequent in the summer (June~August), as shown in Figure 4(b), accounting for 94% of the total. Most events occurred in June, followed by July and August. The seasonal transition phases showed large changes in the number events, such as from May to June and from August to September.

The above analysis demonstrated that the strong convective activity in Xinjiang was obviously higher in the summer than in other seasons, leading to more precipitation. This finding is in line with the climatic background of the monthly precipitation distribution in most parts of Xinjiang. In terms of the temporal MCS distribution, M_βCSs were distributed more widely than M_αCSs. Therefore, in a typical wet season in arid and semiarid areas, short-duration heavy rainfall was caused mainly by M_βCSs.

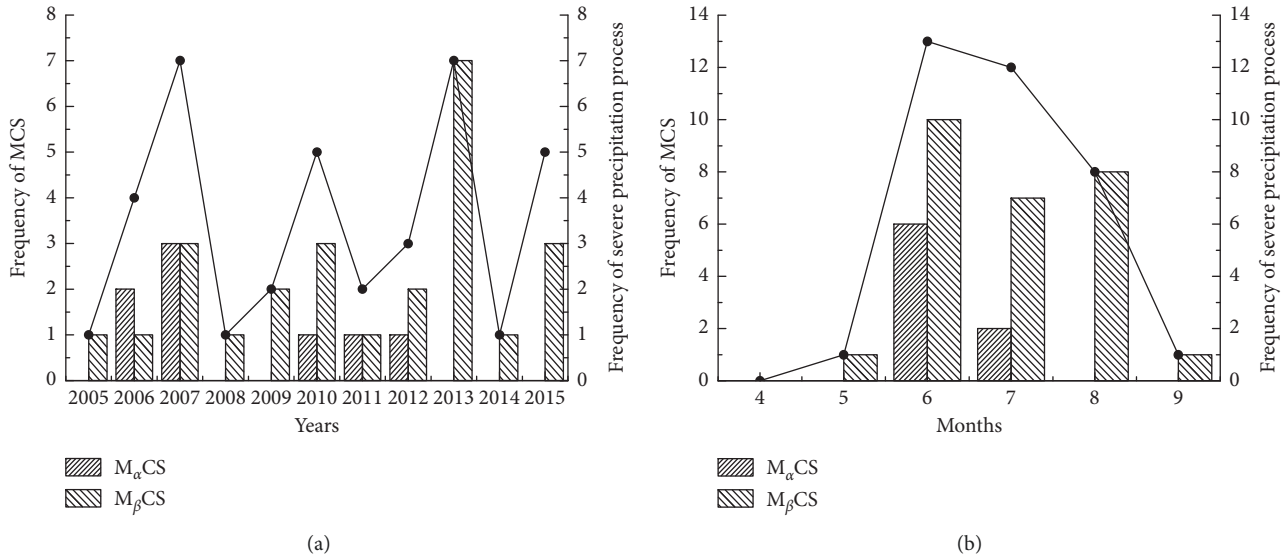

Figure 4: Frequency variations among MCS events of different scales and heavy precipitation processes: (a) annual variations; (b) monthly variations.

The diurnal variation characteristics of MCSs from formation to dissipation showed that the primary period of formation for M_βCSs was from 05:00 to 10:00 and at 13:00 and that the primary period of formation for M_αCSs was from 06:00 to 08:00. These results indicate that MCSs began to appear in the afternoon along with high temperatures; then, the heat-induced convection developed rapidly, which was conducive to the formation of convective clouds with abundant water vapor. The temperature from early morning to midmorning was relatively low, resulting in weak convective activity and lower MCS frequencies (Figure 5(a)).

In terms of diurnal frequency, the maturity period (Figure 5(b)) of M_βCSs showed a bimodal distribution, increasing from 08:00 to 11:00, achieving its maximum value, and then decreasing. After 15:00, the frequency reached a high value again, and the values from 19:00~07:00 of the next day were low. From 10:00 to 12:00 and at approximately 14:00, M_αCSs reached their maturity period, which basically coincided with the occurrence times of the M_βCS frequency extremes. Thus, the MCS area reaches its maximum value in conjunction with the daily maximum temperatures. Because of the long daylight exposure in the spring and summer in Xinjiang, there were still increasing convective clouds at 16:00.

Figure 5(c) shows a multipeak distribution in the dissipation period of MCSs. The dissipation phase was concentrated between evening and midnight and occurred later than the primary formation and maturity phases, specifically at 14:00 and from 16:00 to 18:00. At this time, the Gobi-based surface temperatures decreased significantly. In contrast, in the mountains and in the Tianshan basin in the vicinity of oasis areas, the decrease in temperature lagged behind and convective development was still observed during the first half of night and began to dissipate after midnight, leading to secondary peak at approximately 22:00.

The lifespan distribution of the MCSs (Figure 6(a)) ranged from 3~14 h. The duration of M_αCSs was relatively scattered and ranged from 6~14 h, with durations of 14 h being more common. The M_βCS lifespan distribution was not as broad as that of the M_αCS events, being more concentrated within 7~11 h.

Figure 6(b) shows the distribution of the MCS lifespans. The figure shows that, in June, the MCS events present a triple-peak distribution at 3 h, 6~9 h, and 14 h. In July, the MCSs maintain relatively uniform time-frequency distributions, but 6~9 h and 9~11 h lifespans were more common in August. During the other months, MCSs appeared less frequently, and the lifespans were not apparent.

To gain a better understanding of the characteristics of the features of each phase of the MCSs, the period from formation to maturity is defined as the development stage, and the period of maturation to dissipation is defined as the dissipation stage. Because of the concentration of MCS events from June to August, only the summer is investigated. Based on the data shown in Figure 7(a), MCS development phase exhibited durations ranging from 2~9 h, with a higher concentration within 3~6 h, although a few events exhibited durations of 10~12 h.

In June, the MCS dissipation phases exhibiting durations of 2~8 h accounted for more than 85% of the total, with durations of 6~7 h being the most common (Figure 7(b)). The durations in July and August were shorter, ranging from 2 to 5 h, indicating the dissipation accelerated gradually.

Figure 7(c) shows the frequency distribution of both stages. The x-axis of the figure ranges from 2~12 h. For the development stage, the frequency of 3 h duration accounts for 1/3 of the total. Similarly, for the dissipation stage, most MCSs dissipated quickly over 2~7 h, and most dissipation stages lasted for 3 h. The above analysis illustrates that, in this arid and semiarid area, most of the MCSs develop and dissipate rapidly, resulting in precipitation events with short

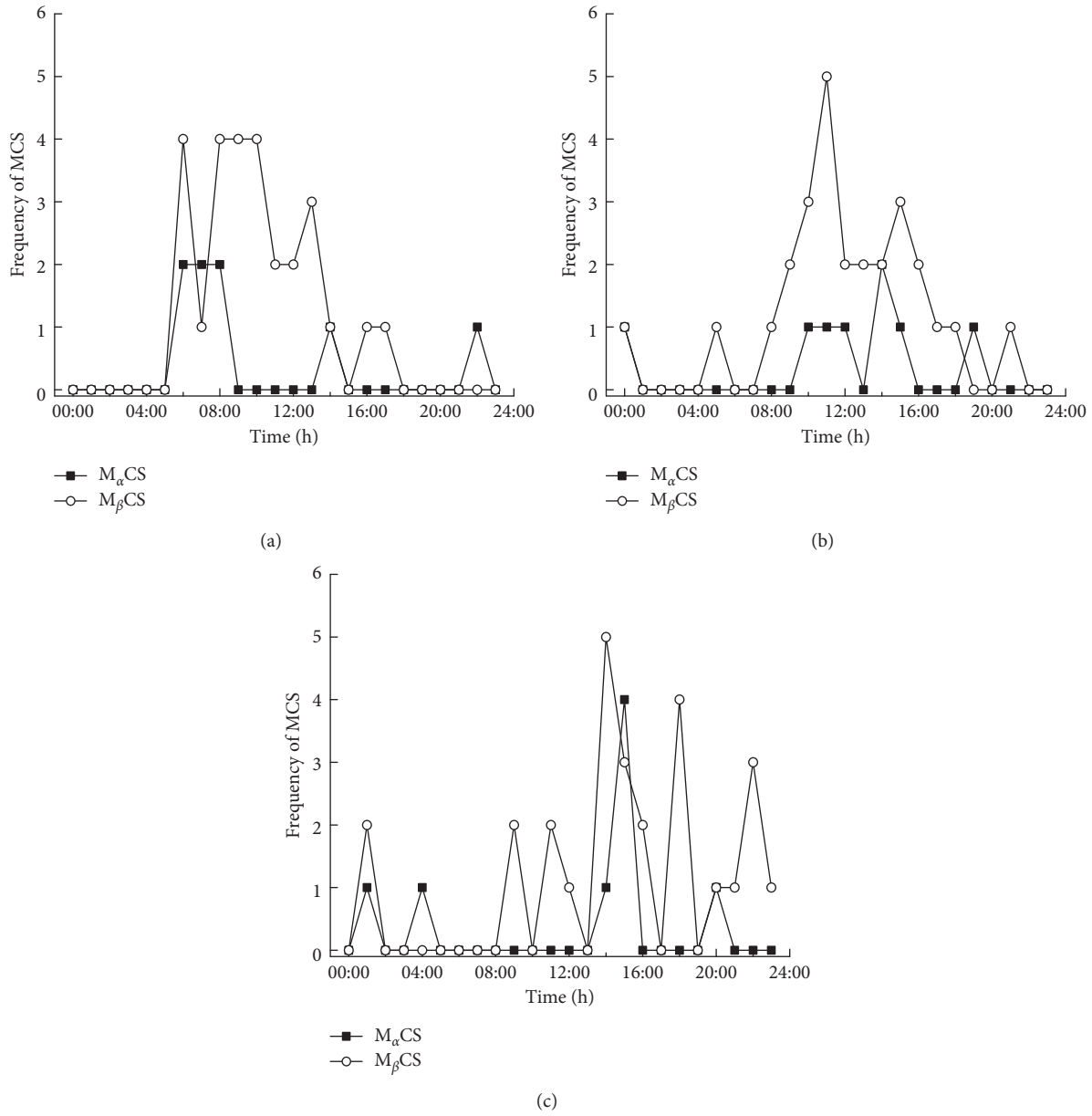

Figure 5: Diurnal frequency distribution of different phases of MCSs: (a) formation; (b) maturity; (c) dissipation.

durations and high rainfall intensity. This finding confirms the fact that short-duration heavy rainfall was dominant in summer of Xinjiang.

Generally, in summer, MCSs occurred frequently in Xinjiang, especially in June and July for M_αCS and all summer months for M_βCSs. The formation period of the MCSs ranges mainly from the late afternoon to evening, and the maturity period mostly occurred in the evening. However, the dissipation period was concentrated in the evening and the first half of the night. The lifespan of MCSs ranged from 3~14 h, and the durations of most M_αCSs and M_βCSs were 14 h and 7~11 h, respectively. Based on the monthly distributions of MCS lifespans, MCSs lasted 6~9 h in June and July and 9~11 h in August. Most of the MCSs featured development stages lasting 3~6 h and dissipation stages lasting 2~7 h. The lifespans of MCSs were closely related to underlying surfaces and temperature changes in this arid and semiarid area. The MCSs developed after the temperature rose rapidly in the afternoon with increased convection, especially over topographically variable surfaces. Accompanied by the movement of different scales, the TBB value of MCSs in the satellite imagery decreased gradually, producing local short-duration heavy precipitation processes.

4.4. Spatial Distribution of MCSs. From the spatial distribution of MCSs in the formation phase (Figure 8(a)), MCSs associated with short-duration heavy rainfall processes were mainly distributed in the vicinity of mountains or mountainous areas and were less common in the basin. In addition, these MCSs were still mainly located within the

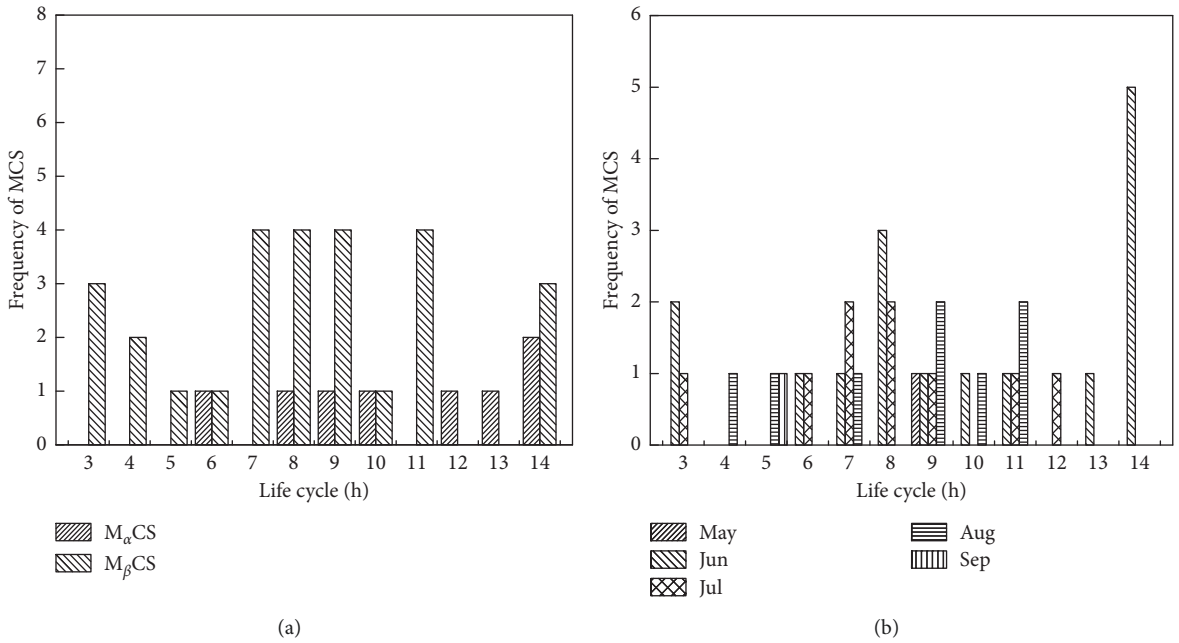

Figure 6: The lifespan distribution of MCSs (a) at different scales and (b) in different months.

territory of Xinjiang instead of in other areas. M_αCSs appeared mainly on both sides of the Middle Tianshan Mountains and to the north and south of the Tianshan Mountains. The most intensive source of M_βCSs was in the Dzungarian Alatau, which is located to the north of the Tianshan Mountains, followed by the Baruch Mountains near the city of Karamay in the low-elevation mountainous region and the southern Tianshan Mountains in the area of Akesu Prefecture. The above phenomena can be explained as follows: influenced by northwestern or western airflow, cold and warm air masses intersected in the West Tianshan or the southern Tianshan Mountains. With the dynamic lifting and relatively abundant water vapor, local convection occurred extremely easily, leading to the formation of MCSs.

Figure 8(b) shows the geographical distribution of MCSs in the mature phase. As seen from the graph, MCSs moved generally eastward, and the distribution was more uniform than that in the formation period. M_βCSs were mainly distributed in the Yili Valley of the West Tianshan and the area along the Northern Tianshan; a small number were also present in the southern Tianshan. However, M_αCSs were more scattered in the mature phase, and the occurrence frequency was higher in northern Xinjiang than in southern Xinjiang in general.

The main dissipation region for M_βCSs was situated in the Gobi oasis transition zone at the edge of the Junggar basin, near Alataw Pass, and in the middle of Akesu Prefecture (Figure 8(c)). M_αCSs appeared concentrated in the Junggar basin, Tarim Basin close to the Tianshan Mountains, and the sides of the Yili Valley.

The analysis to the distribution of MCSs in different phases showed that MCSs mostly formed on the windward slope of mountains or in low mountainous areas, with more MCSs forming on the northern and western portions of the Tianshan than on the southern and eastern portions of the Tianshan. The MCSs then reached maturity over the Junggar basin and dissipated along the edges of the Junggar basin due to dry air in the underlying surface and little moisture supplement from lower layers. As the MCSs moved from the oasis to the Gobi, the convective clouds dissipated gradually.

In the southern Tianshan, MCSs often appeared in western Akesu, and in the northern Tianshan, they often appeared over the low mountainous areas of Bayingol Mongolian Autonomous Prefecture because these two areas were adjacent to a pass. When cold air enters the pass and meets the warm air in low layer of the Tarim Basin, atmospheric instabilities arise, and MCSs are triggered.

4.5. MCS Tracks. As seen from Figure 8, the MCSs were basically generated in the mountains. Located in the middle latitudes, the upper air was strongly influenced by the westerly wind in Xinjiang. Therefore, most of the MCS appearing in the North Tianshan and Junggar basin were from west to east. In the area of Dzungarian Alatau, some of MCSs moves eastward, others proceeded northward and dissipated to the west of Baruch Mountain. MCSs in the southern Tianshan generally moved with the airflow from the southwest to the northeast or north, entering the plain area of the Yili River Valley before dissipating.

Generally, in the context of severe weather processes, MCSs basically moved along the direction of the atmospheric circulation, but some abnormal tracks affected by the specific topography occurred.

5. Discussion

This paper studied MCSs of different scales associated with short-duration heavy precipitation processes. The temporal

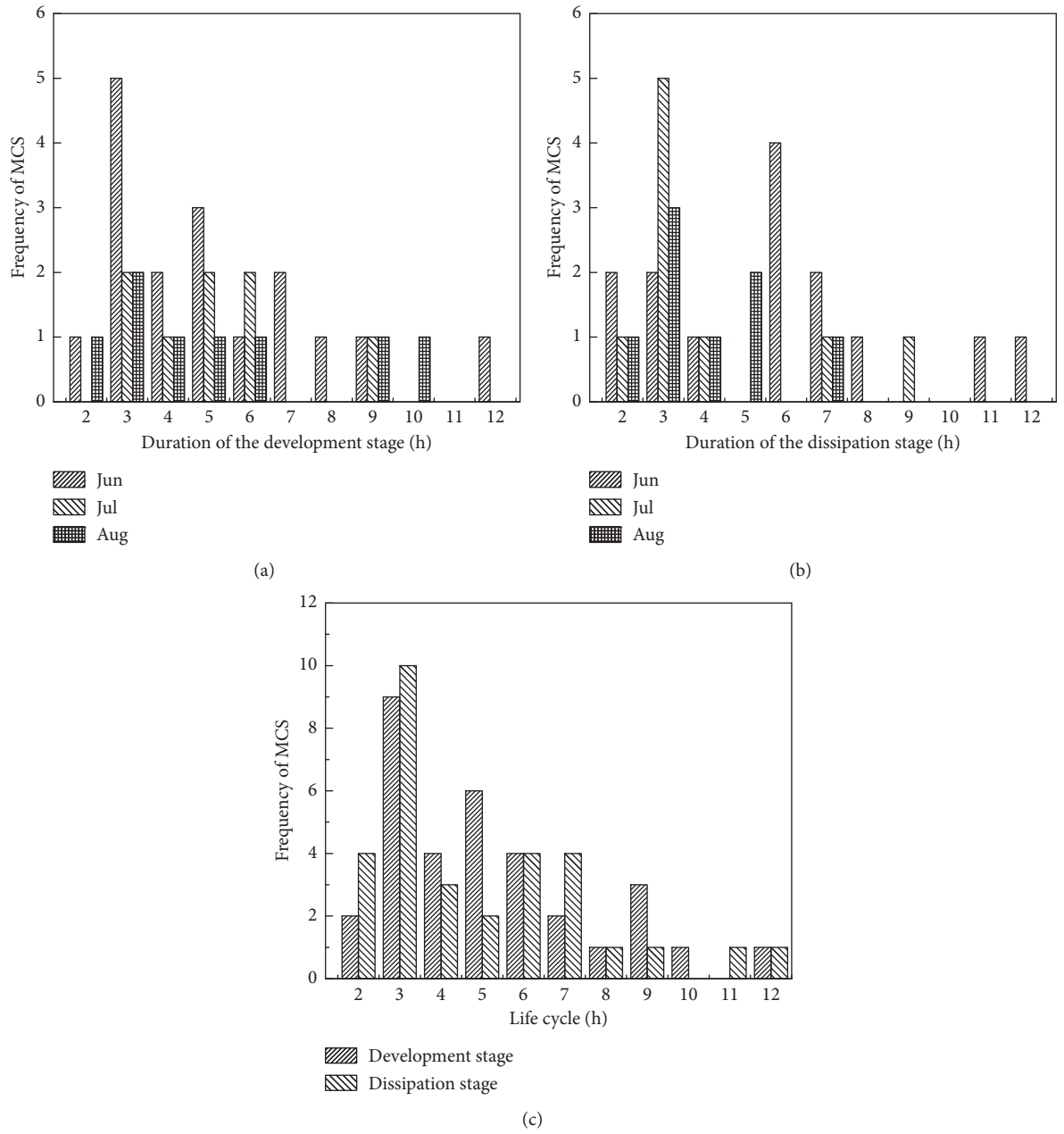

Figure 7: Frequency distribution of the MCSs in every month and the total durations of the (a) development and (b) dissipation stages. (c) Total frequency distribution of both stages.

distribution characteristics of MCSs in the Tianshan region were similar to those in the Yellow Sea area in the summer [27]. The duration of MCSs in the Tianshan region was longer than that in the Sichuan and Chongqing regions but slightly shorter than that in the Jianghuai area [28].

Because Xinjiang is an arid and semiarid region in China, MCSs samples are relatively limited according to the statistics of national short-duration heavy precipitation standards. Thus, the analysis results have certain limitations, so work in the future should focus on short-duration heavy precipitation standard development for the Tianshan region based on the distributions of the hourly precipitation, which may lead to an increase in the sample number and provide the basis for further understanding of the effect of climate change on the development of MCSs.

6. Conclusions

Based on the MCS survey of the short-duration heavy precipitation process in the Tianshan Mountain area over the past 10 years, the temporal-spatial distributions of MCSs in each development period have been analyzed:

(1) Summer was the high-incidence season of MCSs in the Tianshan Mountain area; M_{α}CS appeared most frequently in June, and M_{β}CSs appeared most

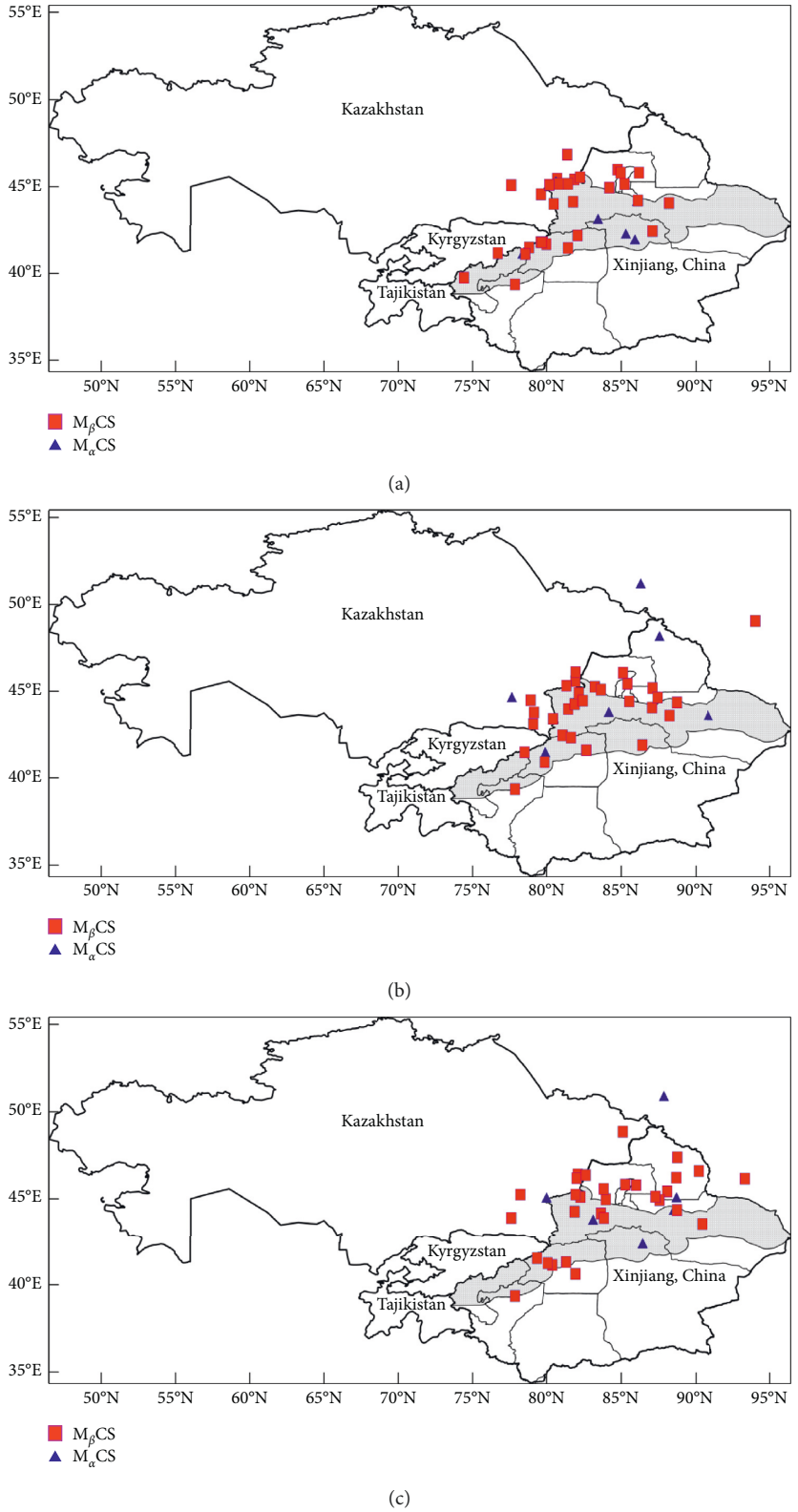

FIGURE 8: Spatial distribution of MCSs in the different stages: (a) formation, (b) maturity, and (c) dissipation (the shaded area represents the Tianshan Mountains and the adjacent area in Xinjiang).

frequently in July and August. The elongated MCSs were more common than their circular counterparts, and deep convection appeared easily in June.

(2) From the yearly variations, the trends of M_βCSs were more similar to those of the heavy precipitation process than those of M_αCSs. M_αCSs appeared easily

in June, whereas M_βCSs appeared in every summer month according to the monthly frequency data. Based on the tracking of diurnal changes, MCSs formed from afternoon to evening, matured during the evening, and dissipated from the evening to midnight.

(3) The lifespan of M_αCSs was relatively long, mostly approximately 14 h, while that of M_βCSs was 7~11 h. MCSs generally lasted 6~9 h from June to July and commonly 9~11 h in August. The durations of the MCS phases were 3 to 6 h for the development stage and 2~7 h for the dissipation stage.

(4) MCSs formed mostly over the windward slope of mountains or low mountainous areas, and the occurrence frequency was notably higher over the northern and western portions of the Tianshan than over the southern and eastern portions. Most MCSs matured in the center of the Junggar basin, and M_αCSs move faster than M_βCSs but were more dispersed. In the dissipation stage, MCSs were mainly distributed along the edge of the basin. The majority of MCSs moved from west to east, but some systems were also affected by the underlying topography.

Data Availability

Previously reported FY-2-retrieved TBB data were used to support this study and are available at http://www.nsmc.org.cn/en/NSMC/Home/Index.html. These prior studies (and datasets) are cited at relevant places within the text as References [16] and [23].

Conflicts of Interest

The authors declare that they have no conflicts of interest.

Acknowledgments

The authors are thankful for the assistance and good suggestions of Dr. Li Ru Qi, Dr. Zhang Yun Hui, and other colleagues who took part in this work. This research was funded by the National Key Research and Development Program (2018YFC1507102), Central Public-Interest Scientific Institution Basal Research Fund (IDM2017003), and the National Natural Science Foundation of China (41565003).

References

[1] E. Callen and D. F. Tucker, "Analysis of Rocky Mountain mesoscale convective system initiation location clusters in the Arkansas-Red River Basin," *Atmospheric Science Letters*, vol. 17, no. 7, pp. 392–399, 2016.

[2] J. E. Nachamkin, R. L. Mcanelly, and W. R. Cotton, "An observational analysis of a developing mesoscale convective complex," *Monthly Weather Review*, vol. 122, no. 6, pp. 1168–1188, 1994.

[3] C. A. Leary and E. N. Rappaport, "The life cycle and internal structure of a mesoscale convective complex," *Monthly Weather Review*, vol. 115, no. 8, pp. 1503–1527, 1987.

[4] P. J. Wetzel, W. R. Cotton, and R. L. Mcanelly, "A long-lived mesoscale convective complex. Part II: evolution and structure of the mature complex," *Monthly Weather Review*, vol. 111, no. 10, pp. 1919–1937, 1983.

[5] R. A. Maddox, "Meoscale convective complexes," *Bulletin of the American Meteorological Society*, vol. 61, no. 11, pp. 1374–1387, 1980.

[6] I. Velasco and J. M. Fritsch, "Mesoscale convective complexes in the Americas," *Journal of Geophysical Research*, vol. 92, no. D8, pp. 9591–9614, 1987.

[7] D. Miller and J. M. Fritsch, "Mesoscale convective complexes in the Western Pacific region," *Monthly Weather Review*, vol. 119, no. 12, pp. 2978–2992, 1990.

[8] J. A. Augustine and K. W. Howard, "Mesoscale convective complexes over the United States during 1985," *Monthly Weather Review*, vol. 119, no. 7, pp. 685–701, 1991.

[9] A. G. Laing and J. M. Fritsch, "Mesoscale convective complexes in Africa," *Monthly Weather Review*, vol. 121, no. 8, pp. 2254–2263, 1993.

[10] N. A. Kalinin, A. N. Shikhov, and A. V. Bykov, "Forecasting mesoscale convective systems in the Urals using the WRF model and remote sensing data," *Russian Meteorology and Hydrology*, vol. 42, no. 1, pp. 9–18, 2017.

[11] A. Madhulatha, M. Rajeevan, S. K. R. Bhowmik, and A. K. Das, "Impact of assimilation of conventional and satellite radiance GTS observations on simulation of mesoscale convective system over Southeast India using WRF-3DVar," *Pure and Applied Geophysics*, vol. 175, no. 1, pp. 479–500, 2018.

[12] D. Mitropoulos and H. Feidas, *Use of Global Precipitation Measurement's Satellite Data for the Study of a Mesoscale Convective System*, Springer International Publishing, New York, NY, USA, 2017.

[13] Q. Yang Jr., R. A. Houze, L. R. Leung, and Z. Feng, "Environments of long-lived mesoscale convective systems over the central United States in a convection permitting climate simulation," *Journal of Geophysical Research Atmospheres*, vol. 122, no. 24, pp. 13,288–13,307, 2017.

[14] J.-H. Jeong, D.-I. Lee, C.-C. Wang, and I.-S. Han, "Characteristics of mesoscale-convective-system-produced extreme rainfall over Southeastern South Korea: 7 July 2009," *Natural Hazards and Earth System Sciences*, vol. 16, no. 4, pp. 927–939, 2016.

[15] W. Jung and T.-Y. Lee, "Formation and evolution of mesoscale convective systems that brought the heavy rainfall over Seoul on September 21, 2010," *Asia-Pacific Journal of Atmospheric Sciences*, vol. 49, no. 5, pp. 635–647, 2013.

[16] Y. Zheng, J. Chen, and P. Zhu, "Climatological distribution and diurnal variation of mesoscale convective systems over China and its vicinity during summer," *Science Bulletin*, vol. 53, no. 10, pp. 1574–1586, 2008.

[17] Y. Ma, X. Wang, and Z. Tao, "Geographic distribution and life cycle of mesoscale convective system in China and its vicinity," *Progress in Natural Science*, vol. 5, pp. 583–589, 1997.

[18] J. Zhang and Z. Deng, *An Introduction to Precipitation in Xinjiang*, China Meteorological Press, Beijing, China, 1987.

[19] L. Yang, Q. Yang, and Y. Liu, "Characteristics of the atmospheric moisture cycle over the TianShan mountains," *Climatic and Environmental Research*, vol. 19, no. 1, pp. 107–116, 2014.

[20] F. M. Wang, *Study on Space-Time Distributing Features of Mesoscale Convective System in Xinjiang*, Lanzhou University, Lanzhou, China, 2016, in Chinese.
[21] X. Wang and Y. Ma, "Geographic distribution and life cycle of mesoscale convective system in Xinjiang, China," *Arid Land Geography*, vol. 35, no. 6, pp. 857–864, 2012.
[22] I. Orlanski, "A rational subdivision of scales for atmospheric processes," *Bulletin of the American Meteorological Society*, vol. 56, pp. 527–530, 1975.
[23] Z. Fei, Y. Zheng, Y. Zhang, and H. Wang, "MCS census and M odification of MCS definition based on geostationary satellite infrared imagery," *Journal of Applied Meteorological Science*, vol. 19, no. 1, pp. 82–90, 2008.
[24] Y. Zheng, P. Zhu, M. Chen et al., "Meso-α-scale convective systems over Yellow Sea region during summers of 1993~1996," *Universitatis Pekinensis: Acta Scientiarum Naturalium*, vol. 40, no. 1, pp. 66–72, 2004, in Chinese.
[25] H. Zhang, Y. Wang, and H. Wang, "Analysis on the characteristics of satellite cloud map of all kinds of rainstorms in Zibo," *Shandong Meteorology*, vol. 3, pp. 12–16, 2013, in Chinese.
[26] Y. Xu, *Analysis on Synoptic Scale Characteristics of Summer Mesoscale Connective System in Heilongjiang Province*, Lanzhou University, Lanzhou, China, 2014, in Chinese.
[27] X. Duan, X. Zhang, and M. Xu, "Spatial and temporal distributions of mesoscale convective systems in Yunnan and its periphery areas," *Acta Meteorologica Sinica*, vol. 62, no. 2, pp. 243–250, 2004, in Chinese.
[28] X. Qi and Y. Zheng, "Distribution and diurnal variations of the MCS over sichuan-chongqing area and Yangtze-Huaihe River basin during the summer of 2007," *Meteorological Monthly*, vol. 35, no. 11, pp. 17–28, 2009, in Chinese.